PAPER

Theoretical Assessment of Ocean Current Energy Potential for the Gulf Stream System

AUTHORS

Xiufeng Yang
Kevin A. Haas
Hermann M. Fritz
Georgia Institute of Technology

ABSTRACT

The Gulf Stream system features some of the fastest and most persistent currents in the Atlantic Ocean and has long been identified as a promising target for renewable ocean current energy. This study investigates the theoretical energy potential of ocean currents for the Gulf Stream system. A simplified analytical model is calibrated and utilized to represent the quasi-geostrophic balance in the North Atlantic subtropical circulation. The effect of turbines is included in the model as additional turbine drag force. The energy equation in the system is derived and analyzed both locally and basin-wide. Basin-wide, energy production from surface wind stress is balanced by energy dissipation from natural friction and turbines. However, the pressure gradient is playing an important role in redistributing the energy in the local energy balance. It is found that increasing turbine drag does not necessarily increase total energy dissipation from turbines. The maximum energy dissipation by turbines is estimated to be approximately 44 GW, although electrical power output will be significantly reduced due to various engineering and technological constraints. The turbine drag has significant impact on the circulation system. The reduction of energy and volume fluxes in the circulation is featured for different levels of turbine drag. It is found that residual energy flux along the western boundary can be significantly reduced under the peak energy dissipation by turbines, while reduction of volume flux is less extreme.

Keywords: Gulf Stream system, ocean current energy, energy dissipation by turbines

Introduction

Surging energy consumption in recent years together with increasing public awareness of environmental protection has spurred growing interest in renewable energy from the ocean (Vanek & Albright, 2008). Ocean currents are an attractive resource of renewable energy due to their inherent reliability, predictability, and sustainability. The general ocean circulation is a combined result of forces including wind stress, Coriolis force, pressure gradients, temperature and salinity differences, friction, and interactions with shorelines and the seabed. Besides these, tides, river discharge, and surface atmospheric pressure gradients also play roles in shaping the currents (Leaman et al., 1987). In most basins, ocean circulations exist in the form of ocean gyres representing large rotating currents. In the North Atlantic ocean, due to the rotation of the spherical earth and westward trade winds, the subtropical gyre is pushed toward the west side of the basin resulting in pile-up of water mass along the eastern boundary of the continent. The westward trade winds in the tropics and the eastward westerlies at midlatitudes exert a clockwise friction and thus a negative curl on the ocean surface, resulting in the equatorward Sverdrup Drift (Sverdrup, 1947). The widely known Gulf Stream system is formed by the equatorward depth-integrated flow returning northward in the western boundary. Western boundary currents are narrower and deeper than the eastern boundary currents and can be 10 times faster and carrying five times as much water (Gross, 1993). The Gulf Stream within the Florida Strait has an ocean current speed exceeding 2 m/s (Hanson et al., 2011).

Various ocean current energy assessment studies have been performed for the Gulf Stream. The earliest systematic research programs on ocean current energy assessment for the Gulf Stream date back to the 1970s. A research project named "Coriolis Program" predicted that an amount of about 10 GW of hydrokinetic power could be extracted from the Gulf Stream using turbines (Lissaman, 1979). A more conservative prediction made by Von Arx et al. (1974) suggests an amount of up to 1 GW kinetic energy can be extracted from the Gulf Stream by turbine arrays without seriously disrupting climatic conditions. However, neither author elucidated on the details of their resource estimates. Recently, Duerr and Dhanak (2012) considered a fraction of the undisturbed power density in the Gulf Stream as equivalent to the available power potential

and estimated that to be in the range of approximately 20–25 GW.

According to the National Research Council (NRC, 2013), the first level of assessments provides estimates of the theoretical resource as the maximum level of resource extraction possible given the feedback associated with energy removal. Power density-based approaches are useful for identifying high-energy regions and preliminary estimates of energy resources for a single or a small number of devices, as long as there is a negligible change to the existing flow. However, power density only characterizes the undisturbed kinetic energy transport by the flow, but not the generation rate of energy by turbines. A large number of devices can block the flow and reduce the current velocity, thereby reduce the generated power from each device. To incorporate the effect of reduced flow velocity that results from the presence of turbines, it is desirable to study the dynamics of the system in order to estimate the theoretically extractable energy. Analytical dynamic models for estimating power potential from tidal streams (Garrett & Cummins, 2005) and atmospheric jet streams (Miller et al., 2011) have already been proposed. Unfortunately, successful analytical models of a similar nature do not yet exist for open ocean currents. Although tidal currents and open ocean currents share obvious similarities, they are fundamentally different regarding their dynamic mechanisms. Tidal stream currents are primarily driven by head difference between the entrance and exit of the channel, while ocean currents are in quasi-geostrophic balance and driven primarily by surface wind stress. The present study is dedicated to filling in this knowledge gap and providing a simplified theoretical estimate of recoverable energy resources from the Gulf Stream system.

The Model

Although forces such as temperature and salinity gradients play important roles in the general circulation of the oceans, the surface ocean circulation is primarily driven by surface wind (Wunsch & Ferrari, 2004). Therefore, the present study only considers the wind-driven circulation with friction, while all other forces are neglected. Energy extraction using underwater turbines can also be considered as energy dissipation from turbines in addition to natural dissipation. Therefore, it is beneficial to first investigate the energy balance in the circulation. Csanady (1989) estimated that the total energy dissipation from the western boundary current in the North Atlantic is approximately 70 GW. Wunsch (1998), considering wind as the major energy source of surface currents, concluded that about 20 GW of energy is attributed to driving the wind-driven circulation in the Atlantic. However, these numbers only provide an estimate of the undisturbed natural dissipation rate in the Gulf Stream, and bear high uncertainty.

The analytical model for the present study investigates energy dissipation from added turbines, a more realistic measure of extractable energy resources from the Gulf Stream system. This model is based on the model proposed by Stommel (1948). The computational domain is a simplified rectangular basin with a flat bottom representing the North Atlantic Basin. The positive x direction is eastward, and the positive y northward. The horizontal and vertical extensions of the idealized basin are inspired by the real dimensions of the North Atlantic Basin. Water density is assumed constant, and the flow is assumed steady. In the ocean, the advective terms (nonlinear terms) are much smaller than the Coriolis term (i.e., Rossby number $\ll 1$), and therefore can be neglected (Vallis, 2006). The reduced shallow water quasi-geostrophic equations consist of two horizontal momentum equations and the continuity equation:

$$-fv = -\frac{1}{\rho}\frac{\partial p}{\partial x} + \frac{(F_x + W_x)}{\rho} \tag{1}$$

$$fu = -\frac{1}{\rho}\frac{\partial p}{\partial y} + \frac{(F_y + W_y)}{\rho} \tag{2}$$

$$\frac{\partial u}{\partial x} + \frac{\partial v}{\partial y} = 0 \tag{3}$$

where ρ is the water density, p is the pressure, f is the Coriolis parameter, W_i is the surface wind stress in i direction, F_i is the opposing forces associated with natural friction, turbulence, and possibly turbine drag in i direction (i = x, y). (x, y) are the east-west, north-south axes, and (u, v) are two corresponding horizontal velocity components.

Since the depth of the ocean (on the order of 1 km) is much smaller than its horizontal extensions (on the order of 1,000 km), shallow water approximation and hydrostatic pressure are reasonably assumed. Therefore, horizontal pressure gradients are simplified to the following:

$$\nabla_h p = \rho g \nabla_h \eta \tag{4}$$

where η is the free surface elevation. Under the β-plane approximation, the Coriolis parameter can be approximated as

$$f = f_0 + \beta y \tag{5}$$

where f_0 and β are constants defined as $f_0 = 2\Omega \sin\theta_0$ and $\beta = \frac{2\Omega \cos\theta_0}{a}$ with Ω as the rotation rate of the earth, a as the earth radius, and θ_0 as a reference latitude.

By cross-differentiating the two momentum equations and subtracting, the pressure gradient terms are eliminated, resulting in

$$f\left(\frac{\partial u}{\partial x}+\frac{\partial v}{\partial y}\right)+\beta v=\frac{1}{\rho}\left(\frac{\partial\left(F_y+W_y\right)}{\partial x}-\frac{\partial(F_x+W_x)}{\partial y}\right). \tag{6}$$

The first term of the above equation is eliminated using the continuity equation. The number of unknowns can be reduced by defining a stream function as

$$u=\frac{\partial \Psi}{\partial y}, \tag{7}$$

$$v=-\frac{\partial \Psi}{\partial x}. \tag{8}$$

Boundary conditions require that both velocity components are zero at the basin boundaries, namely no slip and no penetration at the boundaries:

$$u(x,0)=u(x,b)=u(0,y)=u(a,y)=0, \tag{9}$$

$$v(x,0)=v(x,b)=v(0,y)=v(a,y)=0, \tag{10}$$

where a is the basin length in east-west direction and b is the basin width in north-south direction.

The ocean general circulation is primarily governed by the forcing of the wind; therefore, only wind stress is considered as the driving force in this model. The prevailing wind system on the surface of the North Atlantic ocean include easterly trade winds in the tropics and the westerlies in the middle latitude, exerting a clockwise and negative curl on the ocean surface. A convenient way to represent such wind patterns is to assume a sinusoidal wind profile:

$$W_x(y)=-\frac{\tau_0}{H}\cos\left(\frac{\pi}{b}y\right), \tag{11}$$

where H is the uniform depth of the ocean basin and τ_0 is maximum wind stress.

The drag force is commonly assumed to be proportional to the current velocity square, although it can also be assumed to be proportional to the current velocity to simplify mathematics (i.e., the simplest case in Garrett & Cummins, 2005). To keep this model basic, the drag associated with natural friction and turbulence, and possibly turbines is assumed to be linearly proportional to the current velocity. The undisturbed natural drag (i.e., without presence of turbines) is written as

$$\vec{F}=-\frac{C_d\rho}{H}\vec{V} \tag{12}$$

where C_d is the natural drag coefficient and has the dimensions of velocity in the present setting.

Without the presence of turbines, this model essentially simplifies to the Stommel's model. The solution of Stommel's model is also explained in great detail by Stewart (2008). The details of the derivation are skipped here, and the solution becomes

$$\Psi(x,y)=\frac{b^2}{\pi^2}N\left(\frac{1-e^{m_2 a}}{e^{m_1 a}-e^{m_2 a}}e^{m_1 x}+\frac{e^{m_1 a}-1}{e^{m_1 a}-e^{m_2 a}}e^{m_2 x}-1\right)\sin\left(\frac{\pi y}{b}\right), \tag{13}$$

where $M=\dfrac{\beta H}{C_d}$, $N=\dfrac{\tau_0\pi}{\rho b C_d}$, $m_1=-\dfrac{\left(M+\sqrt{M^2+\frac{4\pi^2}{b^2}}\right)}{2}$, and $m_2=-\dfrac{\left(M-\sqrt{M^2+\frac{4\pi^2}{b^2}}\right)}{2}$.

Two velocity components are then found to be

$$u = \frac{b}{\pi} N \left(\frac{1 - e^{m_2 a}}{e^{m_1 a} - e^{m_2 a}} e^{m_1 x} + \frac{e^{m_1 a} - 1}{e^{m_1 a} - e^{m_2 a}} e^{m_2 x} - 1 \right) \cos\left(\frac{\pi y}{b}\right), \tag{14}$$

$$v = -\frac{b^2}{\pi^2} N \left(\frac{1 - e^{m_2 a}}{e^{m_1 a} - e^{m_2 a}} m_1 e^{m_1 x} + \frac{e^{m_1 a} - 1}{e^{m_1 a} - e^{m_2 a}} m_2 e^{m_2 x} \right) \sin\left(\frac{\pi y}{b}\right). \tag{15}$$

Model Calibration

Before the model can be used to calculate energy dissipation, it needs to be calibrated to make sure it reproduces reasonable flow properties. Considering the great complexity and variability of the Gulf Stream system, as well as the simplicity of this analytical model, it is reasonable to calibrate according to only time averaged bulk flow properties, ideally volume flux and kinetic energy flux.

The basin is defined as a = 6,000 km long in x direction and b = 3,142 km wide in y direction. The Coriolis parameter β in the middle latitude is approximately $2 \times 10^{-13} cm^{-1} \text{sec}^{-1}$. The "basin depth" H in this model is not the mean physical ocean depth, but the depth of surface layer primarily driven by surface winds (i.e., Ekman layer). Stommel (1948) proposed the basin depth H = 200 m, maximum wind stress $\tau_0 = \frac{10^{-5} N}{cm^2}$, or 1 $\frac{dyn}{cm^2}$, and natural drag coefficient $C_d = 0.02\left(\frac{cm}{s}\right)$; however, these parameters are further calibrated below.

The calibrated model needs to be able to reproduce most reasonable bulk flow properties including volume flux and energy flux in the selected cross-section on the western boundary that represents the Gulf Stream. In this study, 7 years of Hybrid Coordinate Ocean Model (HYCOM) data are used to calculate the reference volume and energy fluxes. HYCOM is a data assimilative hybrid isopycnal-sigma-pressure, primitive equation ocean circulation model that evolved from the Miami Isopycnic-Coordinate Ocean Model (MICOM) (Bleck, 2002; Halliwell, 2004). The HYCOM-NCODA Gulf of Mexico Analysis (GoMa) data from the HYCOM online database (http://www.hycom.org) are used in this study. HYCOM-NCODA GoMa (HYCOM hereafter for short) has a spatial coverage extending from 18°N to 32°N in latitude and 98°W to 76°W in longitude with a 1/25 equatorial resolution. In the vertical, it has 40 layers.

To ensure the quality of the HYCOM model data, the HYCOM model data in the vicinity of the chosen cross-section is validated against submarine cable data, which runs across the Florida Strait and measures the volume transport through the Florida Strait channel. This measurement is based on the working principle that the flow through the earth's magnetic field induces a voltage in the cable, which after calibration can measure the volumetric flow (Larsen & Sanford, 1985). The Atlantic Oceanographic and Meteorological Laboratory of National Oceanic and Atmospheric Administration provides online cable data from 1982 till present (available on http://www.aoml.noaa.gov/phod/floridacurrent/). Figure 1 shows the location of the selected cross-section in the Gulf Stream system both in a real geographical map and in the idealized ocean basin. Figure 2 shows the time series of volume fluxes through the same cross-section from both HYCOM and cable measurement. The mean volume flux from HYCOM is Q_{HYCOM} = 31.6 Sv, and the mean volume flux measured by submarine cable is Q_{cable} = 31.4 Sv. It demonstrates that the HYCOM data are fairly accurate in predicting the bulk flow properties of the Gulf Stream system.

For different combinations of basin depth H, maximum wind stress τ_0, and natural drag coefficient C_d, the model produces different flow solutions and therefore different volume flux

$$Q = \int \vec{V} \cdot d\vec{A} \tag{16}$$

and energy flux

$$E_f = \frac{1}{2} \rho \int |\vec{V}|^2 \vec{V} \cdot d\vec{A} \tag{17}$$

through the selected cross-section. The goal of calibration is to find model parameters that minimize both $\left| \frac{Q_a}{Q_m} - 1 \right|$ and $\left| \frac{E_{fa}}{E_{fm}} - 1 \right|$, where the a and m subscripts represent analytical and HYCOM results, respectively. Since these quantities do not always reach a minimum for the same combination of parameters, a compromised strategy is to minimize a new parameter called the "Error Factor" (E.F.):

$$E.F. = \left(\frac{Q_a}{Q_m} - 1 \right)^2 + \left(\frac{E_{fa}}{E_{fm}} - 1 \right)^2. \tag{18}$$

Figure 3 shows the variation of $E.F.$ as a function of model parameters. Results show basin depth H = 140 m, wind stress $\tau_0 = 1 \frac{dyn}{cm^2}$, and natural drag coefficient $C_d = 0.021 \frac{cm}{s}$ lead to the optimal model performance in terms of undisturbed volume and energy fluxes in the Gulf Stream cross-section.

Energy Balance

When turbine drag is added, energy dissipation will be comprised of natural dissipation and dissipation by turbines, a fraction of which

FIGURE 1

Location of the selected cross-section (red line) in the Gulf Stream system, through which volume flux and energy flux are calculated and compared: (a) the North Atlantic Basin (upper) and (b) the simplified basin with analytical streamlines from Equation 13 (lower). (Color versions of figures are available online at: http://www.ingentaconnect.com/content/mts/mtsj/2013/00000047/00000004.)

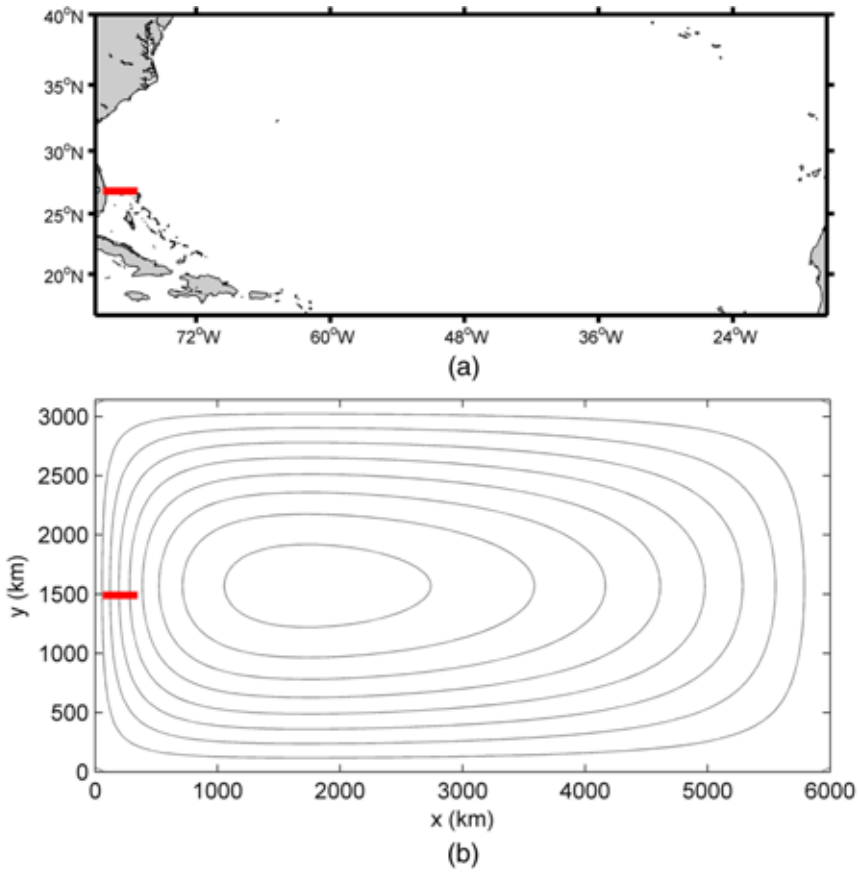

can be collected by turbines and converted into electricity. The presence of turbines is incorporated in the model as additional turbine drag. Similar to natural drag, the additional turbine drag $\vec{T}$ is assumed linearly proportional to current velocity in the following form

$$\vec{T} = -\frac{C_t \rho}{H}\vec{V} \tag{19}$$

where C_t is the turbine drag coefficient and, similar to C_d, has a dimension of velocity. The total drag force in the model becomes $\frac{(C_t + C_d)\rho}{H}\vec{V}$. The solution of the flow has the same form as the no turbine case, except that C_d is replaced with $(C_d + C_t)$ in Equations 14 and 15.

The mechanical energy equation may be found by multiplying Equations 1 and 2 with horizontal velocity components u and v and adding them together, eliminating the Coriolis terms, resulting in

$$-\frac{u}{\rho}\frac{\partial p}{\partial x} - \frac{v}{\rho}\frac{\partial p}{\partial y} + \frac{F_x + W_x}{\rho}u + \frac{F_y + W_y}{\rho}v = 0. \tag{20}$$

Substituting Equations 11 and 12 for the wind stress and drag force into above equation and including turbine drag, we get the following mechanical energy balance equation:

$$-\left[uH\frac{\partial p}{\partial x} + vH\frac{\partial p}{\partial y}\right] - \left[\rho C_d\left(u^2 + v^2\right)\right] - \left[\rho C_t\left(u^2 + v^2\right)\right] - \left[\tau_0\, u\cos\left[\left(\pi\frac{y}{b}\right)\right]\right] = 0. \tag{21}$$

FIGURE 2

Time series of volume fluxes through the selected cross-section from both HYCOM and the submarine cable measurement.

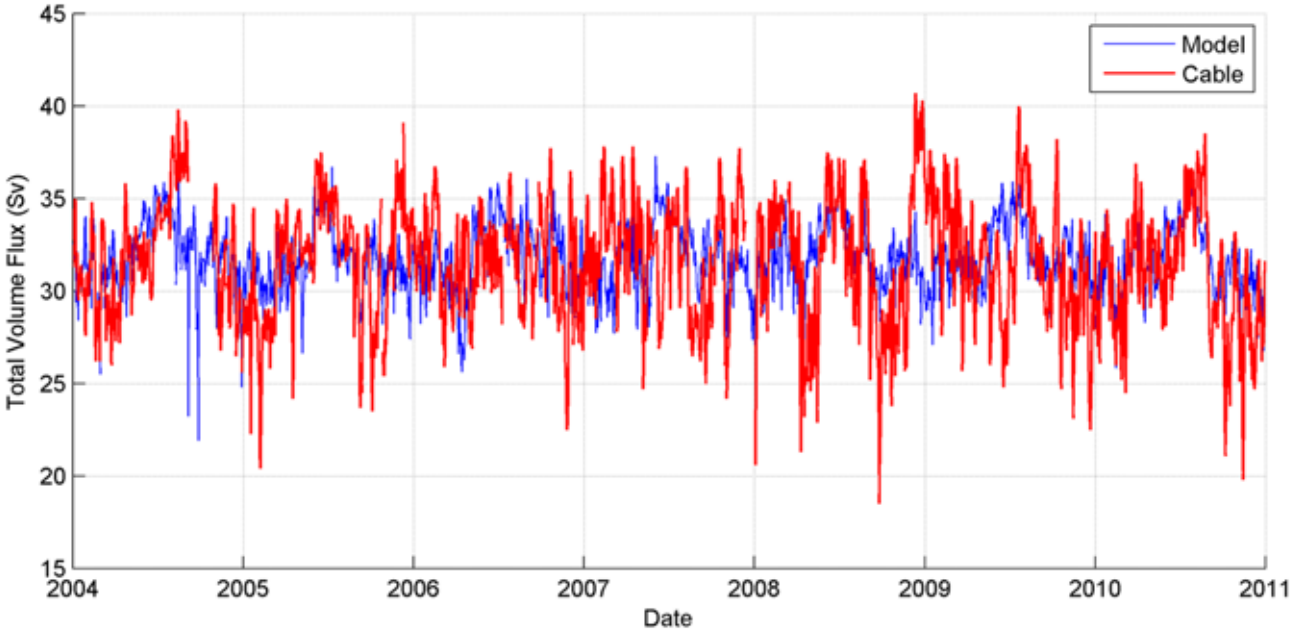

The four terms in the above equation are work done by pressure gradient P_{pres}, natural dissipation $D_{natural}$, energy dissipation by turbines $D_{turbine}$, and the energy production from surface wind stress P_{prod}, respectively. The dissipation terms are all negative indicating a loss of energy whereas the production term is positive indicating a gain in energy. The ocean basin is considered a closed system, and Equation 21 is integrated over the entire

FIGURE 3

(a) Error Factor (E.F.) as a function of varying maximum wind stress τ_0 and natural friction coefficient C_d for different depth (left) and (b) E.F. minimum as a function of depth (right).

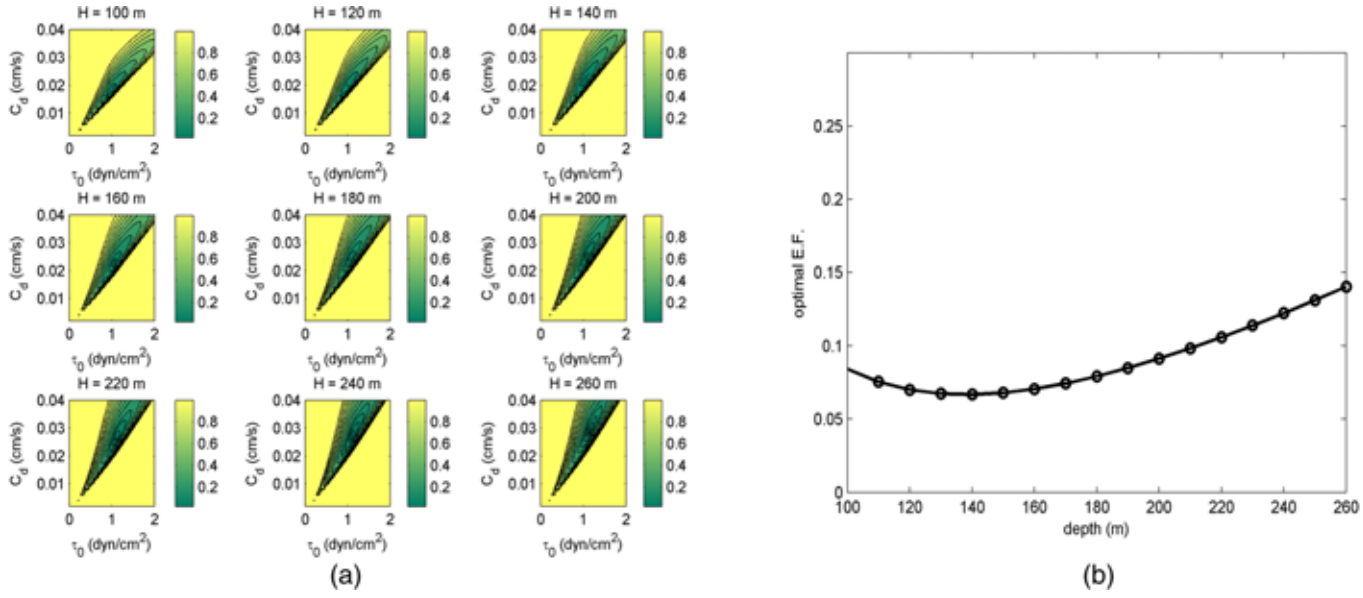

domain. By substituting the solutions from Equations 14 and 15 into the following integration, it is found that

$$\int_{x=0}^{a}\int_{y=0}^{b}\left[-\rho C_d\left(u^2+v^2\right)-\rho C_t\left(u^2+v^2\right)-\tau_0\, u\cos\left(\pi\frac{y}{b}\right)\right]dx\,dy=0. \tag{22}$$

Therefore, we also have

$$\int_{x=0}^{a}\int_{y=0}^{b}\left[u\,H\frac{\partial p}{\partial x}+v\,H\frac{\partial p}{\partial y}\right]dx\,dy=0. \tag{23}$$

Equations 22 and 23 essentially mean in this closed circulation system, energy is solely produced from wind stress (P_{prod}) and dissipated from natural dissipation ($D_{natural}$) and turbines ($D_{turbine}$). Work by pressure gradient P_{pres} only serves to redistribute energy in the basin but does not produce or dissipate energy.

The turbine drag coefficient C_t would typically be a function of the number, spacing, and size of the turbines. Intuitively, the greater this turbine drag coefficient, the stronger energy extraction will be and the more energy dissipation occurs. However, due to the simplicity of the present model, no explicit relationship between turbine drag coefficient C_t and particular turbine properties exists. Although increases in the turbine drag coefficient can be thought of as adding more turbines or increasing their size thereby further dissipating the flow field and reducing the velocity. The flow speed $|V|=\sqrt{u^2+v^2}$ as well as the total energy dissipation from turbines are indirect functions of C_t:

$$\int D_{turbine}(C_t)dA=-\int C_t\rho|V(C_t)|^2dA. \tag{24}$$

Therefore, the total energy balance from Equation 22 in the circulation system is rewritten as

$$-\int\tau_0\cos\left(\pi\frac{y}{b}\right)u(C_t)\cdot dA=\int C_d\rho|V(C_t)|^2dA+\int C_t\rho|V(C_t)|^2dA. \tag{25}$$

The left-hand side represents the energy production, and the right-hand side the energy dissipation. In Equation 25, as C_t increases, current velocity in the circulation will decrease due to increased friction, which will reduce the left-hand side term (i.e., energy production by wind stress) and hence the sum of two terms on the right-hand side (i.e., total dissipation in the system).

Effects of Turbine Dissipation

The total energy dissipation by turbines is shown in Figure 4 as a function of turbine drag coefficient C_t. The red curve corresponds to the case with calibrated model parameters. Model parameters have also been perturbed around their calibration values to show the range of energy dissipation changes. The trend of energy dissipation from turbines is very obvious. When no turbines are included (i.e., turbine drag coefficient $C_t = 0$), the ocean current is undisturbed and energy dissipation by turbines is zero. At the same time, the natural dissipation is at its highest ($\cong 94\ GW$). This number is not far from the estimate by Csanady (1989), which is about 70 GW. As the turbine drag coefficient C_t increases from zero, the energy dissipation by turbines also increases until C_t reaches about 0.04, where energy dissipation from turbines D_t reaches its highest ($\cong 44\ GW$). As C_t increases to beyond 0.04, D_t decreases with C_t, which means adding more turbines will not result in more total dissipation from turbines, but simply further blocks the current flow. Physically, it is because, although the number of turbines increases, the energy dissipation from each turbine decreases. As the turbine drag increases, the natural dissipation rate decreases monotonically.

It is seen that maximum total energy dissipation by turbines is achieved when turbine drag coefficient is about twice of the natural drag coefficient. This essentially means increasing the basin dissipation by about a factor of 3 produces the limiting result corresponding to about twice as much energy dissipation by the turbines as is dissipated naturally. However, it is important to note that the total dissipation under this scenario is actually less than the undisturbed natural dissipation without any turbines because of the increased total drag coefficient.

It is also beneficial to look at the spatial variation of each component in the local energy balance shown in Equation 21. Figure 5 shows the spatial variation of each term from Equation 21 with no turbines ($C_t = 0$). In this condition, no energy is dissipated from turbines (Figure 5a), and all dissipation is in the form of natural dissipation (Figure 5b). Most of the natural dissipation occurs on the western boundary, where the currents are the strongest.

FIGURE 4

Calibrated total energy dissipation by turbines (red) and by natural friction (blue) as functions of turbine drag coefficient; maximum wind stress $\tau_0\left(\frac{dyn}{cm^2}\right)$ and natural drag coefficient $C_d\left(\frac{cm}{s}\right)$ are perturbed around calibrated values to give an envelope of the range of energy dissipation by turbines.

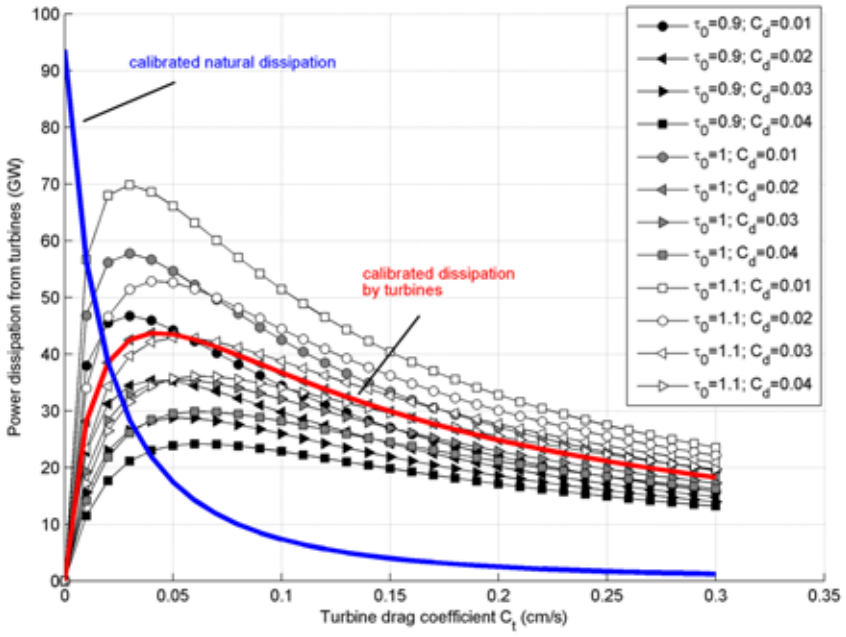

FIGURE 5

Spatial variation of each term from Equation (21) with no turbines: (a) density of energy dissipation by turbines ($D_{turbine}$), (b) density of natural energy dissipation ($D_{natural}$), (c) density of energy production by wind (P_{prod}), and (d) work done by pressure gradient (P_{pres}).

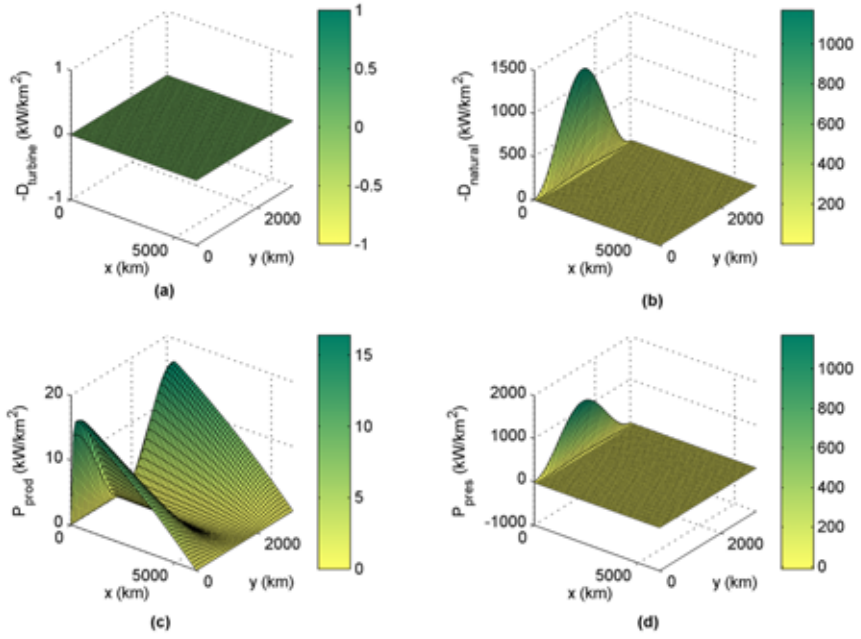

Energy production by wind is the highest on the northern and southern boundaries and fairly weak elsewhere (Figure 5c). Obviously local energy production by wind stress and local energy dissipation are imbalanced, and therefore work from pressure gradient P_{pres} is needed for the local energy to remain balanced (Figure 5d). It is already verified in Equation 23 that the pressure gradient has no contribution to the total basin-wide energy balance but functions to redistribute energy so that energy is locally balanced. This is highlighted on the western boundary, where energy production from wind stress is fairly weak while the energy dissipation is the highest. Therefore, it is both the wind stress and the pressure gradient that sustain the high level of energy dissipation along the western boundary.

Figure 6 shows the same spatial variation of each term from Equation 21, but with the maximum level of energy dissipation by turbines (C_t = 0.04). Energy dissipation by turbines is no longer zero, and natural dissipation is reduced. Energy production by wind stress slightly decreases and the western boundary broadens. It is also noticed that even though additional turbine drag is uniformly applied to the entire basin, most of the energy dissipation by turbines occurs within about 100 km of the western boundary. Therefore, the energy dissipation by turbines from present study provides a reasonable first approximation of energy dissipation by turbines only within the western boundary.

In perfect geostrophic flow, Coriolis force is balanced by pressure gradient, and flow is directed parallel to lines of constant pressure. In the case of quasi-geostrophic flow, although friction is considered, the nature of the pressure gradient counterbalancing the Coriolis

FIGURE 6

Spatial variation of each term from Equation (21) with turbines (C_t = 0.04): (a) density of energy dissipation by turbines ($D_{turbine}$), (b) density of natural energy dissipation ($D_{natural}$), (c) density of energy production by wind (P_{prod}), and (d) work done by pressure gradient (P_{pres}).

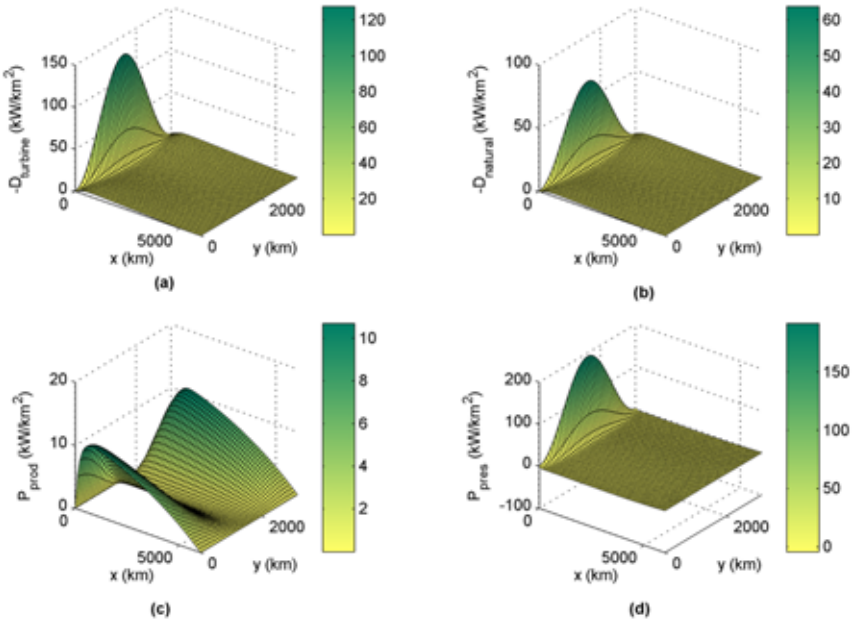

force is still dominant. Figure 7 compares the surface elevation in the basin with no turbines (Figure 7a) and with turbines that correspond to maximum $D_{turbine}$ (Figure 7b). It is seen that, as turbine drag is applied, the water surface is flattened. The surface elevation gradient in x direction $\frac{\partial \eta}{\partial x}$ along the western boundary is significantly reduced, resulting in a reduced pressure gradient $\frac{\partial p}{\partial x}$. Despite the decrease in total dissipation, the Coriolis force fv in the x direction at the same region is correspondingly reduced due to the reduced pressure gradient forcing resulting in much weaker currents. Potentially, this implies the additional turbine drag may slightly raise the sea level in Florida and lower it in the Bahamas.

The effects of turbines can be evaluated in terms of the changes in streamlines as shown in Figure 8 and in residual kinetic and volume energy fluxes at different cross-sections of the circulation with different levels of energy dissipation by turbines as shown in Figure 9. With no turbines (C_t = 0), the flow is in undisturbed state. The western boundary cross-section (θ = 0°) has the highest energy flux passing through, approximately 24 GW. As the angle increases from 0° to 50°, the kinetic energy flux decreases mildly. As the angle increases beyond 50°, the residual kinetic energy flux decreases more rapidly with the angle. When the turbine coefficient is C_t = 0.01, about 28 GW of power is dissipated from turbines, and the residual energy flux in the circulation is

FIGURE 7

Ocean surface elevation with lines of constant pressure: (a) case without turbines (left) and (b) case with turbines (C_t = 0.04) (right).

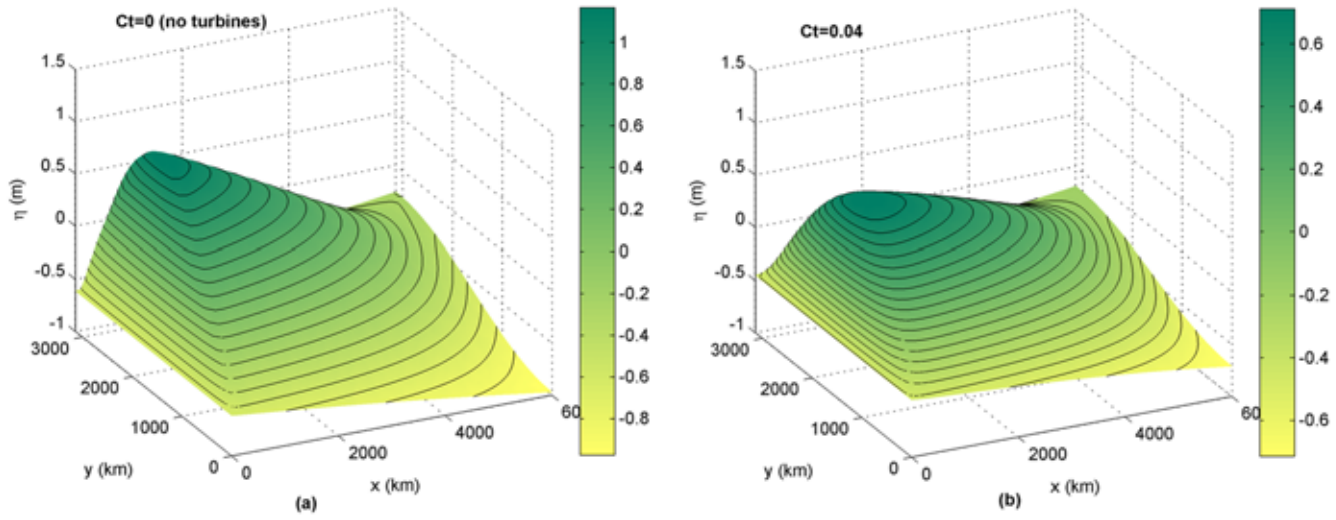

FIGURE 8

Streamlines of the circulation: (a) Undisturbed with multiple cross-sections every five degrees (left) and (b) with turbines (C_t = 0.04) (right).

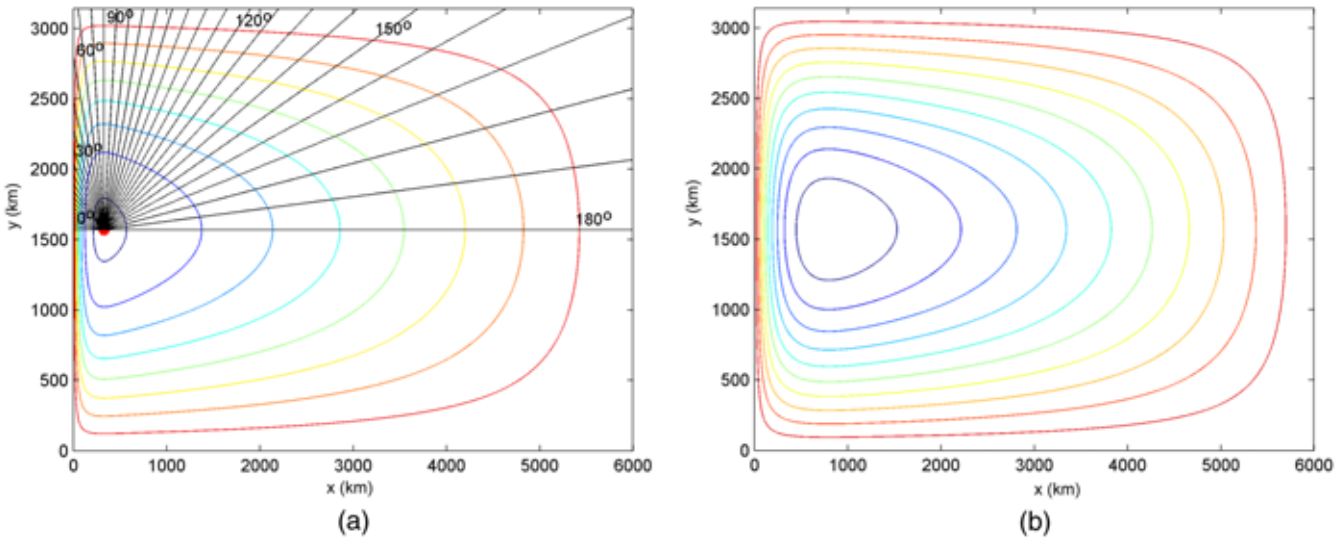

reduced. The residual energy flux through the western boundary cross-section drops to about 7.8 GW, about one third of the undisturbed level (Figure 9a). However, the residual volume flux only drops to about 21 Sv from the undisturbed level of about 23 Sv (Figure 9b). As more turbines are added and the turbine drag coefficient increases to C_t = 0.02, approximately 38 GW of power are dissipated from turbines. At the same time, the residual energy flux on the western boundary drops to about 3.3 GW, approximately 14% of undisturbed level. The residual volume flux drops to about 18 Sv. If we further increase the turbine drag coefficient to C_t = 0.04 so that energy dissipation by turbines is maximized, the residual energy flux through the western boundary cross-section drops to about 1 GW or 4% of the undisturbed (Figure 9a). The residual volume flux goes down to about 15 Sv. Further increasing C_t will not generate more dissipation by turbines but further reduce the residual fluxes. It should be noted that the decrease in residual volume flux is likely due to the uniform turbine dissipation.

FIGURE 9

(a) Residual energy flux for each cross-section defined in Figure 8 with different levels of energy dissipation from turbines (left) and (b) residual volume flux as a function of turbine drag coefficient C_t (right); C_t that corresponds to maximum dissipation by turbines is marked with red dash line.

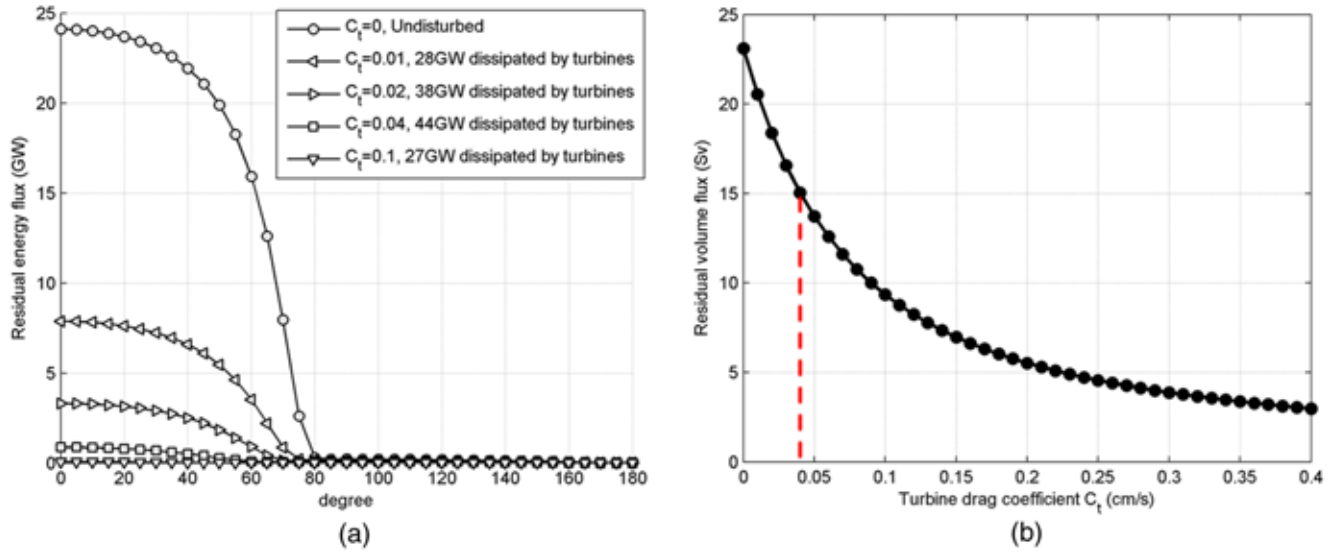

In reality, if dissipation were to only occur in the region with strongest currents, i.e., along the western boundary, there is likely to be little change to the overall volume flux.

Summary and Conclusions

In this paper, Stommel's model is utilized to represent the quasi-geostrophic balance in the subtropical ocean circulation in the North Atlantic. This analytical model is calibrated against 7-year averaged HYCOM model data to ensure it reproduces reasonable bulk flow properties on the western boundary. In this circulation system, energy is produced by surface wind stress and dissipated by natural dissipation and turbines, although the pressure gradient is playing an important role in redistributing energy. Turbines are represented in the model as additional drag, applied to the entire domain to facilitate mathematical manipulation. It is estimated the system can sustain energy dissipation by turbines up to approximately 44 GW at a turbine drag coefficient twice as big as the natural drag coefficient. Increasing the turbine drag coefficient further will not result in more energy dissipation from turbines, but only more reduction in residual flow. When the energy dissipation from turbines is maximized, the residual energy flux on the western boundary is significantly reduced to about 4% of the undisturbed level. The reduction of residual volume flux is less extreme partly due to the widening of the western boundary.

The kinetic energy flux along the western boundary is much higher than elsewhere due to the Coriolis effect. Therefore, most of the energy dissipation occurs along the western boundary even when a uniform turbine drag is applied. Although the energy dissipation by turbines is derived with uniform turbine drag coefficient, it is still a reasonable first approximation of energy dissipation only from the western boundary. However, as defined by NRC (2013), the technically recoverable resource is the resource extraction realizable within the limitations of presently available devices and site-specific resource intensities and should be much less than the theoretical estimate provided here. Such limitations include wake losses, turbine and transmission efficiencies, and other engineering and technological constraints. The exact percentage of the theoretical resource that can be converted into electricity considering Betz's law and turbine related efficiencies needs more research to determine. The typical value of the overall power efficiency is suggested to be around 30% (Behaj & Myers, 2003). Assuming a 30% conversion efficiency from energy removal from the flow to electrical power, turbines yield a peak energy potential for electricity production of about 13 GW from the Gulf Stream system. Further refinement of the resource estimate to the so-called practical resource requires additional constraints such as environmental and economic considerations, which are far beyond the scope of the present paper.

In the future, more accurate estimate of energy dissipation by turbines can be achieved by applying localized turbine drag along the western boundary, a more complicated but more realistic representation of extracting energy from the Gulf Stream system. Analytical solutions may no longer be possible and numerical approaches may be desired.

Acknowledgment

This study was supported by the Department of Energy, Wind and Hydropower Technologies Program award number DE-EE0002661. Any opinions, finding, and conclusions or recommendations expressed herein are those of the authors and do not necessarily reflect the views of the Department of Energy.

Corresponding Author:

Xiufeng Yang
Georgia Institute of Technology
School of Civil and Environmental Engineering
790 Atlantic Drive, Atlanta,
GA 30332
Email: xfyang@gatech.edu

References

Behaj, A., & Myers, L. 2003. Fundamentals applicable to the utilization of marine current turbines for energy production. Renew Energ. 28(14):2205-11. http://dx.doi.org/10.1016/S0960-1481(03)00103-4.

Bleck, R. 2002. An oceanic general circulation model framed in hybrid isopycnic-cartesian coordinates. Ocean Model. 4(1):55-88. http://dx.doi.org/10.1016/S1463-5003(01)00012-9.

Csanady, G.T. 1989. Energy dissipation and upwelling in a western boundary current. J Phys Oceanogr. 19(4):462-73. http://dx.doi.org/10.1175/1520-0485(1989)019<0462:EDAUIA>2.0.CO;2.

Duerr, A., & Dhanak, M. 2012. An assessment of the hydrokinetic energy resource of the Florida current. IEEE J Oceanic Eng. 37(2):281-93. http://dx.doi.org/10.1109/JOE.2012.2186347.

Garrett, C., & Cummins, P. 2005. The power potential of tidal currents in channels. P Roy Soc A-Math Phy. 461(2060):2563-72. http://dx.doi.org/10.1098/rspa.2005.1494.

Gross, M. 1993. Oceanography: A view of Earth, 6th ed. Englewood Cliffs, NJ: Prentice Hall. 446 pp.

Halliwell, G.R. 2004. Evaluation of vertical coordinate and vertical mixing algorithms in the hybrid-coordinate ocean model (HYCOM). Ocean Model. 7(3–4):285-322. http://dx.doi.org/10.1016/j.ocemod.2003.10.002.

Hanson, H.P., Bozek, A., & Duerr, A. 2011. The Florida current: A clean but challenging energy resource. EOS Trans AGU. 92(4):29-36. http://dx.doi.org/10.1029/2011EO040001.

Larsen, J.C., & Sanford, T.B. 1985. Florida current volume transports from voltage measurements. Science. 227(4684):302-4. http://dx.doi.org/10.1126/science.227.4684.302.

Leaman, K.D., Molinari, R.L., & Vertes, P.S. 1987. Structure and variability of the Florida current at 27N: April 1982–July 1984, J Phys Oceanogr. 17:565-83. http://dx.doi.org/10.1175/1520-0485(1987)017<0565:SAVOTF>2.0.CO;2.

Lissaman, P.B.S. 1979. Coriolis program. Oceanus. 22(4):23-8.

Miller, L.M., Gans, F., & Kleidon, A. 2011. Jet stream wind power as a renewable energy resource: Little power, big impacts. Earth System D. 2:201-12. http://dx.doi.org/10.5194/esd-2-201-2011.

National Research Council of the National Academies (NRC). 2013. An Evaluation of the U.S. Department of Energy's Marine and Hydrokinetic Resource Assessments. Washington, DC: The National Academies Press. 154 pp.

Stewart, R. 2008. Introduction to physical oceanography. Open source textbook at http://oceanworld.tamu.edu/. 353 pp. (accessed in 2012).

Stommel, H. 1948. The westward intensification of wind-driven ocean currents. Trans AGU. 29:202-6. http://dx.doi.org/10.1029/TR029i002p00202.

Sverdrup, H. 1947. Wind driven currents in a baroclinic ocean; with application to the equatorial currents of the eastern pacific. Proc Natl Acad Sci. 33(11):318-26. http://dx.doi.org/10.1073/pnas.33.11.318.

Vallis, G. 2006. Atmospheric and oceanic fluid dynamics: Fundamentals and large-scale circulation, Cambridge, UK: Cambridge University Press. 745 pp. http://dx.doi.org/10.1017/CBO9780511790447.

Vanek, F., & Albright, L. 2008. Energy systems engineering: evaluation and implementation. New York: McGraw-Hill. 532 pp.

Von Arx, W., Stewart, H., & Apel, J. 1974. The Florida current as a potential source of usable energy. Proc. Mac Arthur Workshop Feasibility of Extracting Usable Energy from the Florida Current, 91-101.

Wunsch, C. 1998. The work done by the wind on the oceanic general circulation. J Phys Oceanogr. 28(11):2332-40. http://dx.doi.org/10.1175/1520-0485(1998)028<2332:TWDBTW>2.0.CO;2.

Wunsch, C., & Ferrari, R. 2004. Vertical mixing, energy and the general circulation of the oceans. Annu Rev Fluid Mech. 36:281-314. http://dx.doi.org/10.1146/annurev.fluid.36.050802.122121.